JOM
https://doi.org/10.1007/s11837-020-04037-3

Peeling in Biological and Bioinspired Adhesive Systems

BEN H. SKOPIC[1] and HANNES C. SCHNIEPP[1,2]

1.—Applied Science Department, William & Mary, Williamsburg, VA 23185, USA. 2.—e-mail: schniepp@wm.edu

Biological adhesives have inspired synthetically manufactured adhesives with novel properties. Peeling-mode failure is critical to understand these systems and achieve optimal performance. The most common models to describe peeling are briefly reviewed, followed by a literature review of all biological adhesive systems in which peeling plays a critical role, including bioinspired synthetic implementations. From this review, two systems emerge as predominantly studied in this context: gecko feet and spider silk adhesives, both of which are discussed in detail. Gecko feet represent a nanostructured adhesive that has been widely studied because of its unique reversible adhesion and self-cleaning properties. Fibrous and permanent spider silk glues used in spider webs and anchors are interesting given their capacity to withstand hurricane winds and catch and store prey.

INTRODUCTION

The biological world features many examples of adhesives with outstanding performance.[1,2] These systems have inspired the design and manufacture of synthetic adhesives featuring similar properties, especially with application to robotics,[3–5] medicine,[6–11] aerospace,[5] and three-dimensional (3-D) printing/additive manufacturing.[7,12–14] The design and optimization of such bioinspired adhesives can be optimized by studying the failure modes of biological adhesives. Adhesion is a complex multiscale phenomenon,[15] and in many biological adhesive systems such as gecko feet,[16–18] silks,[9,19–21] mollusks,[13,22,23] frogs,[24] and insects,[25–30] peeling is an important failure mode at multiple length scales. Although other adhesive failure modes, such as shearing, generate greater adhesive forces,[31] peeling provides a unique lens through which to study the fundamentals of adhesion, as well as directly assessing or measuring the observable macroscopic adhesion performance of a particular system.[32–34] The present review focuses on peel mode failure, discussing some of the most prominent uses of peeling experiments and corresponding modeling for biological and bioinspired adhesives.

Traditionally, the investigation and characterization of adhesion—particularly in the context of synthetic materials—have focused on the properties of the interface between two materials.[35] Factors that affect the strength of the junction include surface chemistry,[1,36] surface roughness,[35,37–41] junction geometry,[36,42–44] mechanical properties of the materials,[36,44–48] and environmental conditions.[36,49–53] Optimizing these parameters enables the design of highly effective adhesives using epoxies,[43,54–56] polymer films,[46,55,57,58] and other soft surface-conforming materials.[33] Synthetic adhesives developed following this approach have found application in a wide range of regimes.[1,55]

Biological adhesives often feature sophisticated structures optimized through evolution, giving rise to enhanced performance and functionality.[59] The study of these systems has thus significantly expanded the scope of adhesion and provided additional opportunities for the design of bioinspired adhesive systems.[2,59–62] Despite biochemical restrictions in terms of the compounds available via their metabolism, many organisms create adhesive systems with high performance that has not been matched with synthetic adhesives.[1,2,8,12,16,17,19,22,25,63–68] Bioadhesives play a particularly important role in connecting the constituents in hierarchical materials.[59] An example is nacre, a metamaterial with outstanding mechanical performance, which is organized into a layered "brick-and-mortar" structure used by mollusks.[12,22,23] The "bricks" are calcium carbonate ceramic plates, while the "mortar" is made of a variety of elastic biopolymers.[12,22,23] Mollusk-

Published online: 10 February 2020

inspired structures have been synthesized via layer-by-layer 3-D printing to achieve high toughness and strength.[13,69] Nacre is typical of a hierarchically structured biomaterial: a composite material featuring constituents with vastly different mechanical and adhesive properties, featuring a complex structure. Because of their structural and functional complexity, a fundamental study of their adhesive properties based on first principles is challenging.

Given the challenges of developing a fully detailed, fundamental understanding of biological adhesive systems with their structural complexity, a simplified adhesion characterization model is useful and important. Peeling-mode failure is interesting for several reasons: it is simple enough to allow for quantitative analysis, it provides an insight into some of the underlying mechanisms, and it can be directly tested experimentally for intuitive real-life characterization of adhesion performance.[32–34] For wall-climbing animals and many biological composite structures, peeling is the most important failure mode.[17,19,20,70] Peeling-mode failure can provide information about surface energy, elastic/inelastic material response, and behavior under other failure modes, such as lap shear.[32,33,71] Peeling-mode failure for natural adhesive systems is discussed herein from both fundamental and phenomenological points of view. How those natural systems have inspired the design of new engineered materials and adhesives is also discussed. Reviews on peeling in narrower fields, such as spider silk[72] or gecko feet,[16] have been carried out; a review covering the evolution of peeling models[73] has also been published. However, this is the first comprehensive review including peeling in all biomaterials systems and bioinspired adhesives.[16,72,73]

Peeling failure in Nature has been studied in the locomotion of reptiles,[16,18,74,75] amphibians,[24] insects,[29,30] and octopi;[11] in adhesives used in silk architectures;[8,9,21,76,77] and in the intralayer failure of layered composites.[13,78–80] A systematic review of literature reveals that the great majority of studies on peeling in biological adhesives have focused on two systems: gecko feet and spider silk. Gecko feet have received wide attention as a versatile adhesive system with outstanding performance and several other desirable properties. Similarly, adhesion in natural structures made out of spider silk has been widely studied because spider silk is among the biomaterials with best mechanical performance. Following a section that introduces adhesion models, each of these two materials systems is thus discussed in detail in separate sections. In a final section, peeling is reviewed for all other biological systems.

MODELS FOR BIOADHESIVES

One major class of models to describe adhesion using first principles considers the contact mechanics of two elastic spheres. Deformation of this system under compressive load was first described by Hertz in his 1881 work, where he assumed the mechanical properties of the spheres to be homogeneous, isotropic, Hookean, and perfectly smooth.[81] A single elastic sphere in contact with an infinitely rigid and perfectly flat substrate was later considered as a special case.[82] The Johnson–Kendall–Roberts (JKR) model extends the Hertz model to account for adhesion by balancing surface energies of the two materials.[83] As shown in Fig. 1a, this leads to adhesive deformation of the sphere in the contact region, which was not described by the Hertz model. The adhesion creates a negative normal force and introduces hysteresis in the response of the sphere as the force F is applied downward or upward. A mathematical issue with the JKR model is its prediction of infinite stress at the boundary of the contact area. The Derjaguin–Muller–Toporov (DMT) model is a further extension of the Hertz model that adds longer-range attractive forces outside of the contact area, which are approximated using the Leonard–Jones potential.[84] The complexity of this model does not allow for

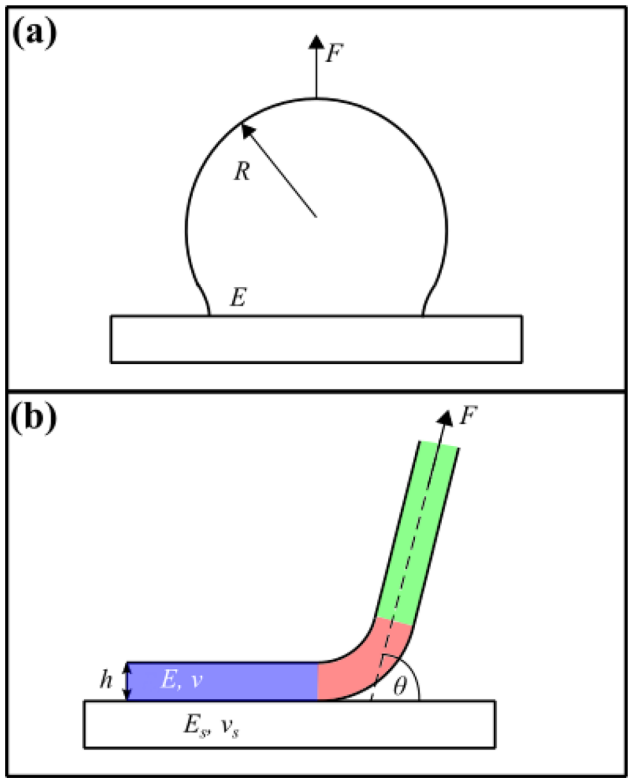

Fig. 1. Two of the leading micro/nanoscale adhesion models. (a) The Johnson–Kendall–Roberts (JKR) model developed in 1971 for spherical elastic solids with high surface energies.[82,83] The model uses a sphere of radius R and modulus E experiencing an applied force, F. Surface energies deform the sphere, increasing the contact area and thus the adhesive forces. (b) The Kendall model developed in 1975 for elastic thin films.[32,34] Peeling force F applied at an angle θ to a thin film with modulus E, Poisson ratio ν, and thickness h attached to a rigid substrate with modulus E_s and Poisson ratio ν_s. Adhered region highlighted in blue, bending region in red, and elastic region in green. The Kendall theory uses a balance of surface, potential, and elastic energy terms (Color figure online).

analytical solutions and requires numerical approaches instead. Muller introduced a dimensionless parameter β to determine whether the JKR or DMT model suits best,[85] defined as follows:

$$\beta = \frac{64}{3\pi}\left[\frac{\gamma^2 R}{\pi E^2 s^3}\right]^{1/3} \quad (1)$$

where γ is the surface energy, R is the radius of the sphere, E is the modulus, and s is the separation. For $\beta \gg 1$, the JKR model is valid. Accordingly, JKR should be applied to large soft materials with high surface energies; DMT should be used for small and stiffer materials, where $\beta \ll 1$.[82] For application to biological systems, this means that the JKR model almost always fits best.[86] The underlying Hertzian assumption of a perfectly smooth surface, however, is quite restricting for real biological systems.

An entirely different geometry is treated by the Kendall model, which describes adhesion of a thin film to a flat surface.[32] As shown in Fig. 1b, a force F is applied to the film at an angle θ. In his 1975 model, Kendall balanced the surface energy created by exposing new area with the work of the applied force and the elastic energy of stretching the film.[32] This model has since been expanded through the contributions of many groups to account for different moduli (E, E_s) and Poisson ratios (ν, ν_s) of the adherend and substrate,[34] yield strength of the film, thickness of the adherend and adhesive,[39,87] bending,[47,71] slipping,[88] prestress,[48] and roughness.[37–39,41,62] While there is a robust understanding of the mechanics of a single thin film peeling from a substrate, application to biological systems requires developing a multiple peeling theory to describe multiple thin films being peeled by a common force.[89,90] A disadvantage of the peeling model is that it is too idealized to be effective for application to complicated systems; for example, the peeling of the legs of many insects involves hair and claws in the adhesion, so modeling it as one elastic thin film is not fully adequate.[25,26,30,91,92]

REVERSIBLE NANOSTRUCTURED ADHESIVE: GECKO FEET

Gecko feet represent the most thoroughly studied natural adhesive system because of its fascinating and unique combination of several desirable properties as a dry adhesive with reversible adhesion on almost any surface and under almost any environmental condition, and self-cleaning and not self-adhering.[16,93] The system requires little attachment or detachment force, yet is impressively strong when adhered.[16,93] These characteristics have made gecko feet the epitome of an ideal adhesive. Gecko feet are also an example of a biological adhesive relying on structural hierarchy: hierarchical levels of setae to spread out to maximize the contact area and thus adhesion strength.[16,17,93,94] Gecko feet have been extensively studied, and while individual properties have been achieved,[3,4,60,61] complete mimicry of all of its natural properties in a single material has not yet been achieved.[16,61,66] Peeling has been critically important for the understanding of gecko feet.[32,34,38,41,50,60,62,70,71,87,89,95–99]

Geckos can adhere to surfaces with their feet, which feature sophisticated hierarchal structures on the bottom of their toes (Fig. 2). The different levels of hierarchy were discovered in different stages, beginning with Cartier in 1872, who saw branches coming off the toes, termed setae (Fig. 2c, d). The advent of electron microscopy allowed Ruibal and Ernst in 1965 to observe the spatular nanostructure at the tip of each seta (Fig. 2e).[16,17] The spatulae are the elements establishing contact with the surface, facilitated by their extreme thinness of only 5 nm to 10 nm. This thinness allows the spatula to conform to the surface over their contact area of $\sim 60\ \text{nm}^2$ by reducing bending and thus maximizing adhesive forces.[39,94,100]

To model the adhesion of gecko feet, the JKR (Fig. 1a)[17,94,100] and Kendall (Fig. 1b)[32] adhesion theories were employed. In one of the first approaches, the JKR model was employed at the larger length scale of an entire seta (Fig. 2d), which was approximated as one deformable elastic solid sphere on a rigid substrate.[17,83] However, this represented an oversimplification of the sophisticated geometry of the foot.[16] A more advanced and fundamental understanding of gecko adhesion requires a model taking into account the smallest hierarchical level of structure: the spatulae (Fig. 2e). Because the area of each spatula making contact with the surface essentially is a thin flat film (Fig. 2f), the Kendall model is ideally suited for their description.[18,100] Early studies also attempted to apply the JKR model to individual spatulae but did not achieve agreement with experimental observations.[16,75,101] This confirmed that film-based peeling models are a better fit for the geometry of the spatulae.

Viscoelastic Pressure-Sensitive Adhesives

Because the spatulae of gecko feet are essentially thin and flat, research on the adhesive properties of gecko feet is closely related to adhesive tapes. The adhesive layer on these tapes is generally classified as viscoelastic pressure-sensitive adhesive (PSA); the viscous characteristics of this material facilitate maximization of the contact area after applying pressure. Like the spatulae on gecko feet, these adhesive layers can be modeled using Kendall peeling theory.[46,57,58,70,102,103] Both systems have been compared theoretically[18,39,48,51–53,62,71] and experimentally.[74,101] The study of viscoelastic PSAs is a broad field with applications in packaging, automotive, electrical, medical, architecture, and engineering fields.[46] The present work focuses on

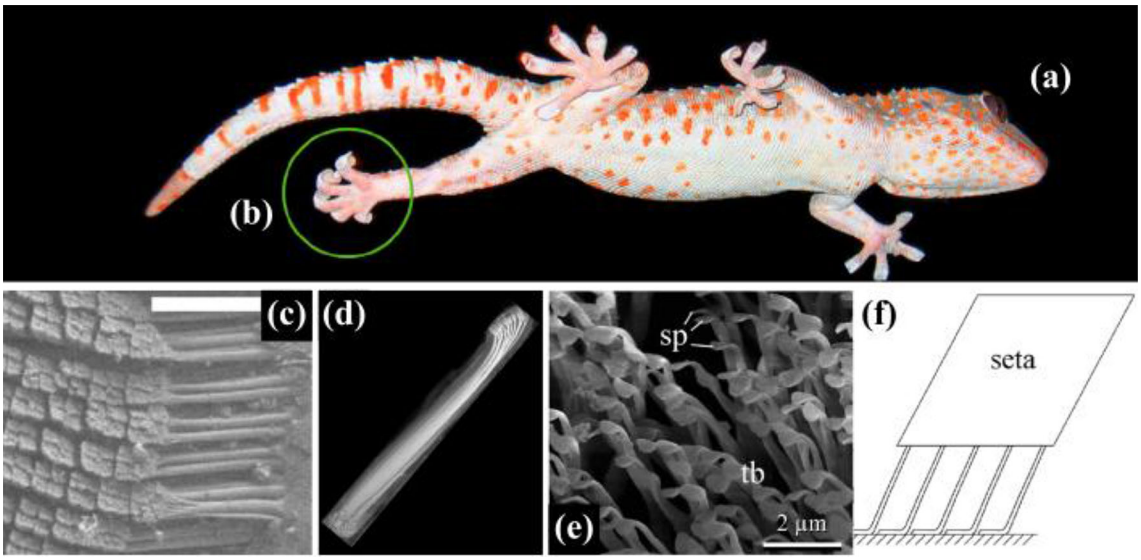

Fig. 2. Hierarchy of the adhesive system of gecko feet. (a) Ventral view of a Tokay gecko (Gecko gecko) climbing a glass surface. (b) Gecko foot peeling from a glass surface. (c) Array of setae in a grid-like pattern. Each diamond-shaped structure is the branched end of a group of four setae clustered in a tetrad. Scale bar: 50 μm. (d) Micrograph of a single seta.[17] (e) Terminal branches (TB) of the setae featuring curved spatula (SP) forming a nanofilm. (f) Diagram showing spatula modeling based on Kendall peeling. This adhesion model has been used to approximate the adhesion of the entire gecko.[48] Permissions: (a)–(d) Adapted with permission of Ref. 17. Copyright 2006 The Company of Biologists. (e) Adapted with permission of Ref. 94. Copyright 2003 American Institute of Physics (f) Adapted with permission of Ref. 48. Copyright 2012 American Institute of Physics (Color figure online).

PSA literature directly used to describe the adhesion of gecko feet.

An important parameter to model thin-film adhesion is the peel angle θ with respect to the substrate, as described in the original Kendall model, shown in Fig. 1b.[32] It has been investigated to model gecko feet to understand why the gecko is able to remove its foot without a measurable detachment force.[16,32] More advanced peeling models also took into account the bending energy in the bent region of the peeled film (red in Fig. 1b). Pesika et al. used such an approach to calculate an optimum peel angle of 18.4° for the gecko, which agrees with experimental observation.[18,104] According to their findings, this ideal angle is dependent on linear modulus, bending modulus, and adhesive strength.[18]

The onset of peeling occurs above a threshold force, and correspondingly, the applied force stretches the material not adhered to the substrate and stores elastic energy in this region (green in Fig. 1b) even before the onset of peeling.[32] In addition to this stretching, there is also a bending region that has been removed from the substrate and curves towards the full peeling angle (red in Fig. 1b). Above the peeling threshold, material newly released from the substrate is also stretched, while the bending region propagates with the peel. Going beyond the original Kendall model, an advanced model by Peng and Chen investigated the energy in this bending region and found that it can be significant even for thin films;[47,71] their model also considers pre-tension in the adhered film. He et al. employed computational analysis considering both the bending and extension effects in a single model.[71] He's model accurately describes PSA mechanics for large strains and further works for small angles, a regime in which the original Kendall model breaks down.[32,71] The work of He et al. is currently the most general peeling model for thin films and can model gecko spatulae satisfactorily, as shown in Fig. 2e and f.

While the thin-film models can correctly predict the experimentally measured pull-off forces of a single spatula of 10 nN,[74,93] more modeling work is needed to include structural features at higher hierarchical levels, and ultimately, the entire gecko. A simple way to scale from an individual spatula to the whole gecko is to multiply the pull-off force of a single spatula by the total number of spatulae on the gecko's four feet. The Tokay gecko has four feet, each with five toes with $\sim$ 20 setal arrays. Each of these arrays features thousands of setae, and each seta has 100 to 1000 spatulae. The corresponding adhesive force for the entire gecko would be 1300 N, approximately the weight of a human. However, this number is far greater than the experimentally measured adhesive force for a gecko, $\sim$ 20 N.[16,93]

Effect of Roughness

Roughness is one of the most important parameters affecting adhesion, commonly quantified using a Greenwood–Williamson (GW) normal distribution.[35] Modeling efforts to describe the response of viscoelastic PSAs to roughness usually consider the interaction of a PSA with a single asperity on an otherwise flat surface.[105] Such a single-asperity

model can be scaled to the entire PSA using the GW distribution. These models have been applied to adhesion of setae.[39,41,62,94]

Persson and Gorb investigated mathematically the effect of fractal roughness on seta-based adhesion.[94] They discussed the influence of the wavelength of periodic substrate roughness in relation to the size of the adherend.[94] Two important parameters came out of their model: the adhesion length, relating relative surface energies with the film's mechanical properties, and the effective interfacial free energy parameter. The adhesion length is compared with the substrate's roughness amplitude to determine whether the adsorbing structure can maintain contact with the substrate.[49,94] Peng and Chen investigated mathematically the effect of periodically rough substrates of sinusoidal[39] and corrugated[41] morphology. Their models use normalized roughness, which is the ratio of amplitude to wavelength.[39,41] They found in both models that the size and stiffness of the film relative to the normalized roughness determine the adhesion strength. Using the sinusoidal model, they found that large stiff films cannot conform perfectly to substrates with large normalized roughness, leading to low adhesion. Short and more elastic films can adhere under a wider range of roughness parameters, because they can make more intimate contact with the substrate.[39] The corrugated model employed the Kendall model to determine angle-dependent adhesion, and found essentially the same results as the sinusoidal model.[41] Despite idealizing the roughness geometry as sinusoidal or corrugated, both models agree with experiment. Huber et al. conducted experiments with live geckos on different substrates to determine the adhesive force. They found their results to be in good agreement with thin-film peeling models predicting the effect of roughness (Fig. 3d). They were the first to develop a spatula-based model that explains the effect of roughness on the adhesion of gecko feet.[101]

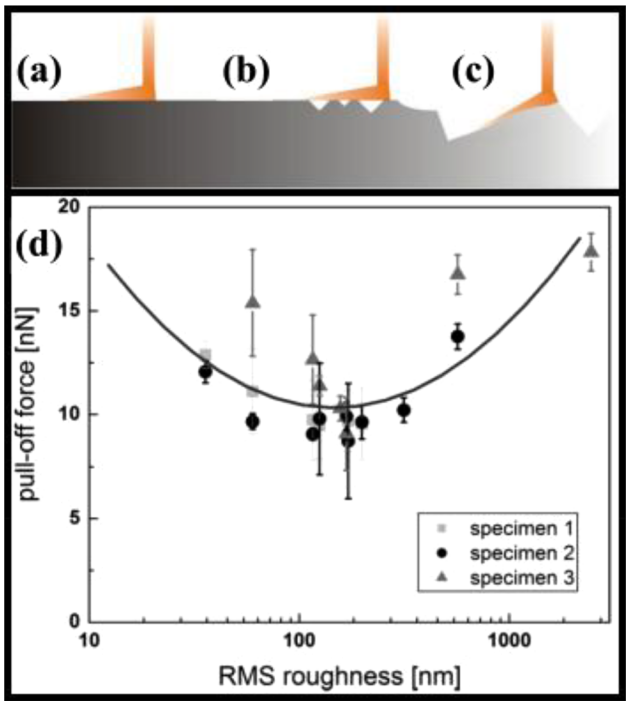

Fig. 3. Model developed by Huber et al. to describe the effect of roughness on gecko adhesion.[101] (a–c) Spatula behavior as a function of roughness. (a) At low roughness, there is intimate contact. (b) As roughness increases, the spatulae are too stiff to conform with the surface, thus making little contact with the substrate. (c) For high roughness, the spatulae can flex and make intimate contact with the substrate again. (d) Experimental results for three Tokay geckos (Fig. 1) in a 25°C and 45% relative humidity (RH) environment. The model describes the experimental results well.[101] Permission: (a–d) Adapted with permission of Ref. 101. Copyright 2007 Acta Materialia Inc. (Color figure online).

Effect of the Environment

Because geckos live in a variety of climates, the effect of water on adhesion has been an area of focus.[106] Experimental reports agree that geckos present significant adhesion in almost all humidity conditions.[50,51,53] In low relative humidity (RH) conditions (RH $\ll$ 70%), van der Waals adhesive forces dominate.[16,74,93,107] When RH increases but remains below 70% (the threshold above which water forms a monolayer), the van der Waals forces decrease. This decrease, however, is overcompensated by an increase of the strong attractive disjoining pressure due to the presence of water, which causes the overall adhesion to increase.[50,51] When RH > 70%, a second layer of water forms on the substrate and water molecules agglomerate under the nanofilm and form droplets. Consequently, van der Waals forces and disjoining pressure forces become negligible.[50,51] However, geckos are still able to adhere even in these environments via capillary forces.[50] Peng and Chen modeled the effect of capillary forces in the adhered and bending regions to describe gecko adhesion in the RH > 90% regime.[50] Under these conditions, water agglomerates under the film and thus also in the bending region. Depending on the interfacial energies of the water/substrate/adherend system, the capillary forces of the meniscus forming on the bending and elastic regions can provide significant adhesive forces.[50] In summary, the mechanism providing adhesive forces changes from van der Waals to disjoining pressure to capillary forces in order of increasing RH.

Temperature has been shown to have a significant impact on the adhesion of viscoelastic PSAs and therefore also on geckos.[1,53,70,102] Peng et al. developed a model that considered the influence of the environmental temperature on peeling and found that peeling strength decreases at higher temperatures, due to a viscosity decrease of the PSA.[53,103] Gent et al. showed that, in addition to the effect of the environmental temperature, there is also an internal increase of temperature caused by friction within the layer peeled off.[103] This effect is

particularly pronounced at high peel rates, where this internal temperature increase becomes comparable to the effect of the environmental temperature. Viscoelastic mechanics, roughness, and environment have all been considered in the design of gecko-inspired synthetic adhesives. In the next subsection, how these parameters have been addressed to more accurately reproduce the outstanding adhesive properties of gecko feet is discussed.

Engineering and Applications

Research on the adhesion of gecko setae and PSAs has inspired engineered adhesion systems. One fundamental characteristic of the adhesion of gecko feet is their hierarchical structure, which increases the adhesive strength and detachment energy (toughness). This was first shown theoretically[91,92] and later by experiment.[60,108] Gorb designed a sample of polyvinylsiloxane (PVS), which was poured through a porous substrate, resulting in a mushroom (MR)-shaped adhesive, as shown in Fig. 4a–d.[60] Gorb conducted Kendall peeling experiments of the PVS samples on glass to determine the adhesion strength, and this adhesive system was found to have twice the peel strength of an unstructured PVS sample, simply by adding the artificial mushroom setae.[60] In comparison with Gorb's work, Murphy created an adhesive with two additional hierarchical levels of mushrooms at smaller length scales, as seen in Fig. 4g–j.[108] Murphy found that each additional hierarchical level increased the strength and toughness of the adhesive. While mushroom-shaped microstructures are relatively simple to make, they have a significant backing behind the contact area and thus do not exhibit the same mechanical characteristics as the much thinner natural spatulae of geckos.[109] Also, the mushrooms have circular symmetry and thus peel uniformly from any direction, in contrast to the gecko, whose spatulae are folded in a particular direction and thus feature a preferred peeling direction.[109]

Daltorio et al. applied the effects of pull-off angle of gecko feet to robotics. They designed and built a quadruped wall-climbing robot named Mini–Whegs™ with four-spoked legs with nonhierarchically structured double-sided Scotch® Magic™ tape for adhesion.[3] The legs were designed to maximize adhesion while minimizing the detachment force by coordinating the peeling angles between the legs.[3] Asbeck et al. engineered a similar robot (Fig. 4k) with a hierarchical adhesive employing the anatomically accurate peel angle discovered by Pesika et al. and designed the robot to perform gecko-like movements.[3,4,18] The hierarchical adhesive featured three layers of thin polydimethylsiloxane (PDMS) films with wedges in successively decreasing sizes. The largest wedge was attached to the robot, and the smallest was the adhered surface, as shown in Fig. 4l and m.[4] Stickybot, shown in Fig. 4k, successfully climbed vertical wood, painted metal, and glass surfaces.

Gecko-inspired adhesives are not limited to robotic wall-climbing systems. Applications have been designed for improved microelectronics,[110] biomedical adhesives,[111] and many more, as the mimicking of these adhesives improves.[66,110,112] Work to mimic the gecko's ability to adhere in diverse environments has also been successful. Saltannia and Sameoto coated a hierarchical structure similar to Fig. 4a–d with polymers featuring different degrees of hydro-philicity. They showed that more hydrophobic polymers saw a smaller reduction in adhesion strength under water.[113] Despite this success, they did not observe the increase in adhesion performance in wet conditions that gecko feet show.[50,106] Yi et al. used hierarchically structured hydrogels as the bioinspired adhesive and were able to achieve strong adhesion in dry, moist, and wet environments.[114] Early efforts with gecko-inspired self-cleaning polymers showed promise in terms of retaining adhesion strength on dirty substrates.[115] To investigate self-cleaning, Alizadehyazdi et al. developed a JKR-based model to determine the adhesion of nanoparticles as a function of their size. They demonstrated experimentally the ability to release the particles from the matrix by applying a centripetal force via spin coating, to emulate repeated gecko foot removal.[116] These advances toward mimicking the adhesion of gecko feet completely are exciting but do not yet match the performance observed in the gecko. One cause is that research has focused on mushroom-shaped microstructures, which are easier to manufacture but do not have the same morphology or mechanics as film-like spatulae.[109] Recent developments in nanoorigami might help to produce hierarchical setae with spatulae in the future.[117] This will allow experimentalists to make hierarchically structured systems mimicking gecko feet better. This approach has the potential to unify the efforts of researchers working on viscoelastic film models with experimentalists trying to engineer an adhesive exhibiting all of the gecko adhesive properties.

PERMANENT, FIBROUS ADHESIVE: SPIDER SILK

Spider silk is one of the most highly performing biomaterials,[7,20,67,118–121] featuring three times the toughness of Kevlar.[119] It has provided much inspiration for designing improved polymer fibers because of its unique material properties.[63–65,118,122,123] Structures made with silk require strong adhesion to leverage this performance. In contrast to gecko feet, reversibility is not required; spider-silk adhesives are permanent, deployed only once. This provides adhesion of silk fibers to prey (glues), to substrates (anchorages), and to other silk fibers (silk–silk junctions). These

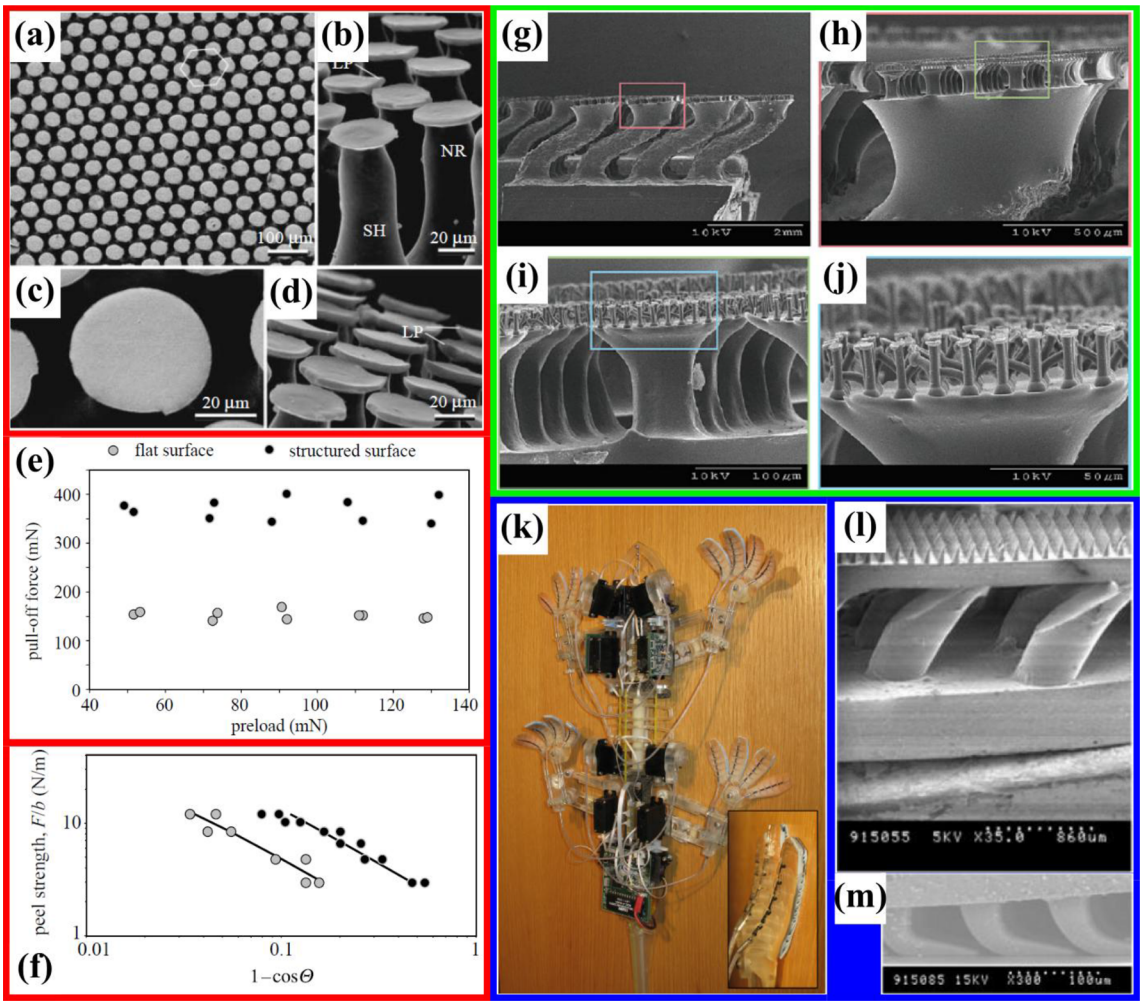

Fig. 4. Gecko-foot-inspired adhesive systems. (a)–(d) SEM micrographs of mushroom (MR)-shaped polyvinylsiloxane (PVS) fibers.[60] (a, c) Top view from above, and (b, d) side view. The structures are 100 μm tall; the tops are 40 μm in diameter and 2 μm thick.[60] (e) Pull-off force from glass versus preload, with and without MR microstructure. (f) Peel strength versus peel angle for PVS, with and without MR structure. The experiment for (e) and (f) was a classical Kendall peel test, showing that the microstructure improved adhesion. (g–j) SEM micrographs of a three-level hierarchical MR-shape adhesive system at increasing magnification revealing all three levels of MRs with diameters of 400 μm, 50 μm, and 5 μm.[108] (k–m) Robotic adhesive system "Stickybot" (k), featuring a hierarchical adhesive modeled after the gecko,[4] shown by SEM (l). (m) One hierarchical level in loaded state. The robot can climb vertical wood (k), glass, and painted metal surfaces. Permissions: (a–f) Adapted with permission of Ref. 60. Copyright 2006 The Royal Society. (g–j) Adapted with permission of Ref. 108. Copyright 2009 American Chemical Society. (k–m) Adapted with permission of Ref. 4. Copyright 2009 IEEE (Color figure online).

adhesives have been observed in both orb-weaving[64,65,77,124,125] and cobweb-weaving spiders.[72,126–128] Viscoelastic glues from orb-weaving spiders form beads on the silk to catch and secure prey in the web.[124,126,128] Glues from cobweb and orb weavers have similar functionality and molecular composition, but only the orb weaver glues are humidity sensitive.[72,125,127,128] Silk fibers need to be mounted firmly enough to make use of their outstanding strength. This is only achieved if they are anchored strongly enough to withstand the fibers' breaking force—and in some cases even hurricane winds[65,129]—without slip or detachment.[65,128] The silk anchorages achieve this by spreading out into hierarchal branches to make many contacts, increasing the contact area and anchor strength.[21,65] Silk–silk adhesive junctions, finally, have been shown to increase the toughness of the web and have inspired engineering of acoustic and mechanical metamaterials.[64,128,130,131]

As in the case of gecko feet, the simple and effective Kendall peel model can be used to determine the materials' adhesive properties. However, because of the complexity of spider webs, the single-tape peel model has been expanded to include multiple tapes coupled by a common force (Fig. 5-e).[89,90] Three categories of spider adhesives are discussed herein; for all three, peeling is an important failure mode, and the peel test is a prominent characterization tool used.

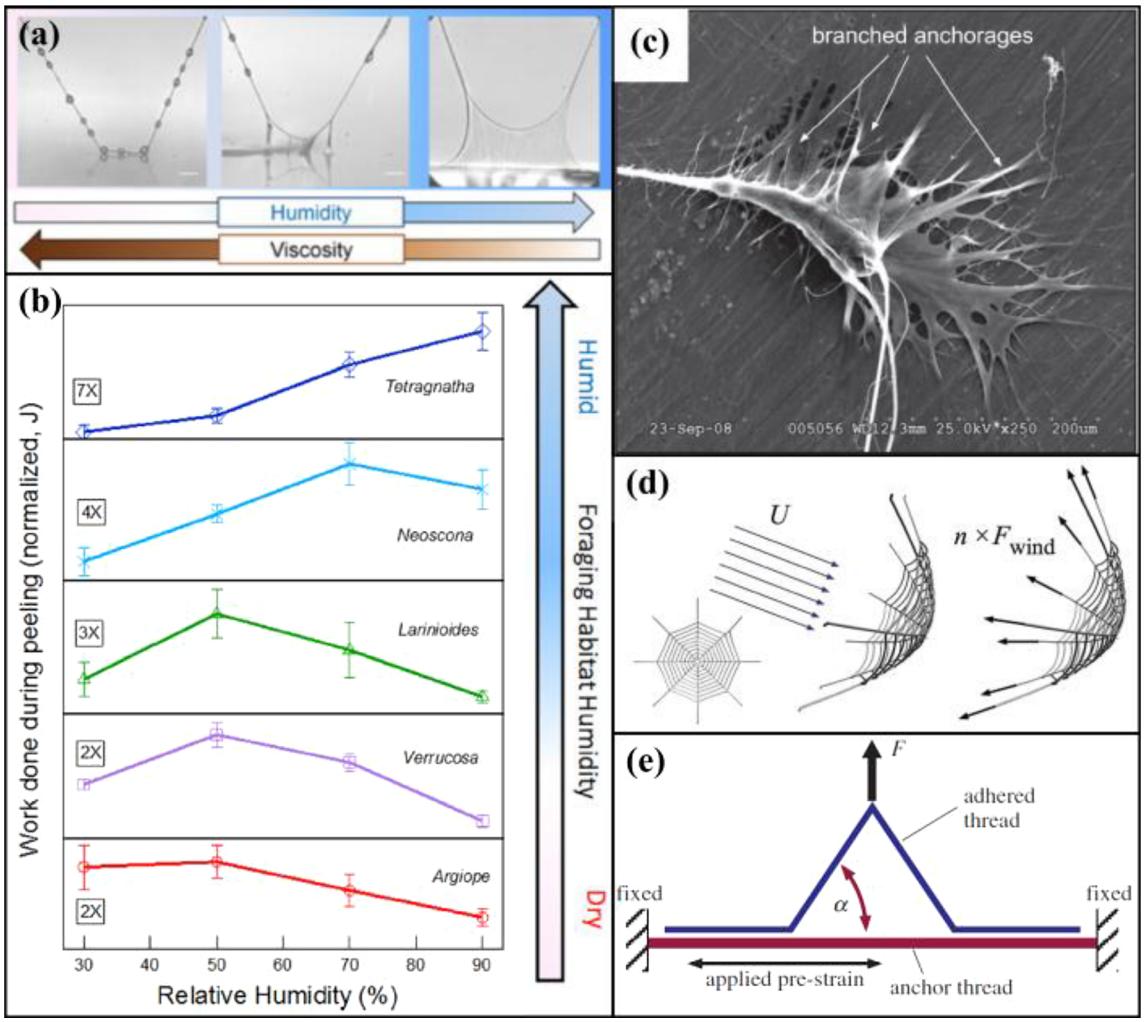

Fig. 5. Application of peeling models and experiments to spider silk adhesives. (a) Silk from a Larinioides cornutus spider pulled at 0.1 mm s^{-1} at low, medium, and high humidity. The glue beads decrease in viscosity and increase in extensibility.[77] (b) Work done during peeling of capture thread from five spider species at four humidities. Humidity of the species' habitats decreases from top to bottom. For each species, maximum adhesion occurs at the humidity closest to the species' natural habitat.[77] (c) Scanning electron microscopy (SEM) image of the attachment disc of a black widow *L. hesperus*, at ×250 magnification.[132] (d) Wind simulation loading the anchorages uniformly, an application of the multiple-peeling model.[65] (e) Ideal model of silk–silk connection with a symmetrically adhered thread attached to a laterally fixed anchor at angle α. Anchor–thread stiffness can be found through stress–strain tests or applied prestrain.[64] Permissions: (a) and (b) adapted with permission of Ref. 77. Copyright 2005 American Chemical Society. (c) Adapted with permission of Ref. 132. Copyright 2009 The American Society for Biochemistry and Molecular Bioloogy, Inc. (d) Adapted with permission of Ref. 65. Copyright 2013 Wiley–VCH Verlag GmbH & Co. (e) Adapted with permission of Ref. 64. Copyright 2014 Royal Society (Color figure online).

Liquid Adhesive

The first category of spider adhesives are liquid adhesives that agglomerate into droplets on the silk fiber. This type of adhesive has been reported for several families of spiders such as the *Theridiidae* (cobweb weavers)[72,127] and *Araneidae* (orb-web weavers).[77,124–126] The liquid droplets consist of water-soluble components, such as peptides and hygroscopic salts, and components not soluble in water, such as glycoproteins and lipids.[72,124,125] The exact composition of these glues varies between *Theridiidae* and *Araneidae*, featuring different properties.[72] *Araneidae* glues are viscoelastic and humidity sensitive because of water-soluble components.[72,77,124,125] These orb-weaver glue droplets feature solid viscoelasticity, providing strong adhesion for prey capture and the ability to hold prey for an extended period of time.[126] *Theridiidae* glues, in contrast, exhibit fluid viscoelasticity and are invariable under changes in RH, despite a similarity of their constituents,[127] which is not yet fully understood.[72]

Araneidae glues increase their volume with increasing humidity, as shown by Opell et al. for a number of *Araneidae* species.[125] The limit of this increase was predictable by the spider's natural habitat (Fig. 5a and b):[125] spiders naturally living in dryer environments saw a limit to droplet size; for increasing humidity, droplets merged (Fig. 5a).[125] Droplet volume and extensibility were found to be positively correlated: larger droplets with more

water have lower concentrations of the chemical constituents resulting in low viscosity and higher extensibility.[125] These trends are visualized in Fig. 5a and b. With high humidity, the droplets combine to form a viscous fluid, rather than the individual viscoelastic spheres observed at low humidities.

It was also reported that higher extensibility correlates with greater stickiness or adhesive strength.[77] For this adhesive system, a peel test was implemented for a strand of silk with many droplets that was attached to a substrate and pulled off with equal tension on each side of the strand (Fig. 5a).[72,77,124,125] Across all *Araneidae* species studied, the peak adhesive work was achieved where the droplets had optimum humidity for their native environment: the point of greatest volume and extensibility.[77,125] In some dry-environment species, an increase in RH results in a decrease of droplet viscosity to the point that adhesion is lost.[72] For engineering systems requiring adhesives suspended along a fiber, we can learn from the *Araneidae* spider silk glue to account for changes in humidity. More work is needed to understand *Theridiidae* glues so that we can learn how to engineer an RH-invariant adhesive for applications in environments with highly variable RH.

Anchorages

Silk anchorages are imperative to web construction for all spiders; to construct a web, spiders must anchor part of the web to a substrate. An example of a silk anchorage from a black widow spider is shown in Fig. 5c. These anchors are found in the iconic orb-weaving spiders, which build picturesque spiral webs, supported by a horizontal and vertical joist in homes. The spirals are made of viscid silk from the flagelliform silk gland, while the radial components giving the structure to the web are made from main dragline silk from the major ampullate (MA) gland.[133] The MA silk is anchored using attachment disc silk from the piriform gland,[132] yet another silk material similar to the glues discussed above.

The attachment discs spread out into a hierarchy of branches to increase the contact area of the adhesive junction.[21,65] These highly branched anchorages led to the development of multiple-peeling theory[89] and later computational efforts.[90,134] The multiple-peeling theory developed by Pugno takes the classical Kendall peeling model and applies it to various geometries inspired by these anchorages of multiple tapes coupled by a common applied force.[32,89,134]

The anchorages have been shown to provide much of the toughness of spider webs,[65] similar to the hierarchical characteristics of gecko feet. Branching of adhesive threads in the attachment disc silk allows the smallest hierarchical level of silk to cover a larger area and make intimate contact with the substrate. The levels of silk hierarchy give the anchor strength and toughness, as spider silk fibers have high toughness.[65] Pugno et al. used the theory of multiple peeling to evaluate an optimal peel angle for the anchor and determined that this is dependent on an interface surface energy parameter.[65] They also determined that, for an entire orb web, the system is self-annealing and finds the optimal configuration and peel angles while under load.[65]

Wolff and Herberstein investigated anchorage response to variable loading directions.[21] They used high-speed filming to observe *Nephila plumipes* spiders in Nature form an attachment disc and determined that it is a two-dimensional (2-D) scanning procedure, which results in 3.5 m to 8 m of piriform silk being laid to form the attachment disc. This leads to the highly intertwined and branching silk anchors observed. They further determined, using Kendall-like peeling experiments, that the attachment discs are constructed to be directionally strong along the main dragline silk direction.[21] This group was the first to determine the spinning process and architecture of the anchorages. Their findings provide a better understanding of the robustness of spider webs, so that static adhesive systems with comparable properties can be designed.

Silk–Silk Adhesion

Silk–silk junctions are imperative for all spider web constructions. One geometry of these junction is parallelly adhered silk fibers that form bundles of fibers.[64] The adhesion is provided by the same glycoprotein glue droplets discussed above.[76,126] The peeling behavior for this system has been described using a two-dimensional modification to the multiple-peeling theory and is similar to a double-peel test, as shown in Fig. 5e.[64,89,96] One silk fiber gets peeled from the other in such a way that one fiber has two peeling regions along the other fiber, but unlike a traditional double peel on a rigid substrate, both fibers experience strain.[33,64] In this peeling system, the adherend and substrate are identical, featuring the same elastic material properties. This is different from the other systems considered so far in this review, in which biological materials (setae or silk) are adhered to a rigid substrate.

The two main types of silks found in orb webs are the radial MA silk and the spiral flagelliform silk.[76] Three silk–silk junctions of an orb web were investigated by Greco et al.: radial-to-spiral, radial-to-radial, and radial-to-substrate (anchorage). They determined that different junctions use different adhesives: radial-to-spiral junctions use the liquid adhesive discussed above; the radial-to-radial and radial-to-substrate use attachment disc silk for adhesion. The radial-to-spiral and radial-to-radial systems might be good candidates for future analysis using the hierarchical multiple-peeling theory.[76,89,134] The junctions using the hierarchically structured attachment silk were much stronger

than the liquid-adhesive junctions. The authors concluded that the difference in junction strength allows the web to maintain strength and toughness by having some sacrificial junctions fail rather than the entire web.[76]

Sacrificial bonding in silk fibers was also reported by Koebley et al., who investigated the looped web structure of the cobweb-weaving Chilean recluse spider *Loxosceles laeta*.[63] Unlike in orb webs, the silk–silk junctions forming the loops do not use any additional adhesive.[122] Unlike the more common cylindrical silk morphology, *Loxosceles* MA silk forming these loops has a flat ribbon morphology that allows the silk to form these junctions with large contact areas. The loops are formed by this spider with a density of 20 loops/mm and increase the toughness of the silk thread significantly.[63] Silk production is energetically demanding for spiders, therefore it is advantageous if their webs last a long time.[14,63,76] Spiders form toughness-increasing structures to allow their webs to be more robust: orb webs for *Araneidae* and loops for *Loxosceles*. The loops have not yet been investigated using peeling theories but would be an excellent candidate. The loops are interesting, since the strongest silk–silk loop junctions fail at about half the tensile strength of the ribbon fiber, without any additional adhesive; importantly, the loops open without damaging the fiber.[63]

Qin et al. printed a 3-D synthetic orb web out of a single elastomeric material: PDMS.[14] To print the webs, they used a direct ink writing technique, which allowed them to vary the thread diameter within the printed web to mimic the radial and spiral types of silk. They determined that the variability in the mechanical properties of the different types of silks[133] gives natural webs their ability to be strong and tough.[14] Through additional modeling and simulation that included these variable thread diameters within the web, they were able to match experimental findings for web loading better.[14] Their finding is similar to the study of Guo et al., which also determined the stress distribution in an orb web.[129] Guo et al. determined the mechanical properties of the different types of silk in the orb web experimentally and applied them to a stress distribution simulation. These works demonstrate that fiber architectures that achieve the same properties as natural webs can be produced.

OTHER BIOLOGICAL ADHESIVE SYSTEMS

Reversible adhesives for locomotion are seen in animals other than the gecko, in many cases also employing hierarchical microstructures.[26] These are seen in insects such as flies,[30] beetles,[25,29,68,135] cockroaches,[28] and spiders with hair-like structures covering their legs (Fig. 6a and b).[26] As in gecko feet, these hairs (setae) provide adhesion by van der Waals forces. Theoretical peeling models have suggested that such hierarchical setal structures can increase toughness.[91,92] However, unlike the spatulae of the gecko, these microstructured hairs do not make intimate contact with the substrate at the near-atomic level, resulting in a major reduction of adhesive forces. Consequently, these hairs typically work in conjunction with claws at the end of their tarsi (legs), mechanically attaching to large asperities on the surface to hold the organism.[28,68] Fundamental modeling or experimental work with individual hairs has not yet been carried out. Experimental studies simplified the complete system to a single peeling adherend to apply thin-film

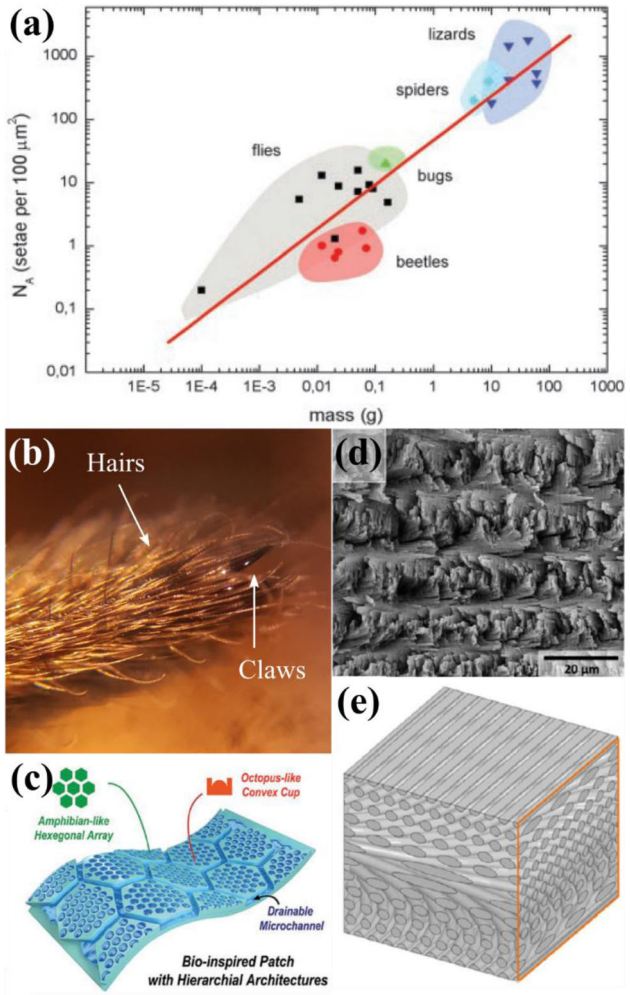

Fig. 6. Other biological and bioinspired adhesive systems that fail by peeling. (a) Density of setae versus mass of the associated organism.[26] The gecko is the heaviest animal capable of maintaining adhesion, because it has the highest density of setae. (b) Optical image of a wolf spider Rabidosa rabida leg with two claws at the end for increased adhesion. (c) Hierarchically structured patch with hexagonal base inspired by frog feet covered by convex suction cups inspired by octopi legs.[137] (d) SEM image of the exoskeleton of crustacean Odontodactylus scyllarus. The Bouligand structure has layers with different planar orientations making at least one complete rotation. (e) Model unit cell of a Bouligand structure with relative planar angles of 16.3°.[141] Permissions: (a) Adapted with permission of Ref. 26. Copyright 2003 The National Academy of Sciences of the USA. (c) Adapted with permission of Ref. 137. Copyright 2019 WILEY–VCH Verlag GmbH & Co. KGaA. (d) and (e) Adapted with permission of Ref. 141. Copyright 2014 Acta Materialia Inc. (Color figure online).

peeling models.[25] Since these models are not a good fit for these geometries, only a phenomenological understanding was obtained. Another microstructured adhesive system is found in the attachment of beetle wings to their bodies.[29] It consists of two complementarily structured surfaces which interlock when in contact. Consequently, this adhesive is strong in tangential/shear mode, yet peels with ease. The Kendall peeling model has been used to validate observations. Somewhat similar to the gecko, this system has inspired the development of synthetic mushroom adhesives.[25,29]

Another reversible adhesive system found in Nature is suction cups, lining the legs of octopi, the mouths of leeches and mites, and the anal regions of mites.[136] Suction cups are predominantly found in aqueous milieu, where deformation of the sucker generates the suction adhesive force. Mites feature a unique air-based system; they secrete a viscoelastic liquid in the sucker cavity to provide the fluid necessary for suction. Similarly, frogs coat their toe pads with an adhesive fluid.[24] Frog toes are covered by hexagonal nanopillars featuring dimples with inverted curvature. Whether or not these structures give rise to suction forces has not yet been determined conclusively. Frog feet were studied using atomic force microscopy (AFM) to determine the topography and mechanical properties of the nanopillars.[24] Kim et al. designed a hierarchically structured adhesive patch inspired by suction cups from octopi and by the hexagonal structures from frogs, which has been shown to be an effective wet adhesive that is strong in peeling-mode failure (Fig. 6c).[137] Suction cups are effective wet adhesives and thus have played a larger role than gecko feet in inspiring medical applications.[138]

Finally, peeling-mode failure is studied in intralayer mechanics of layered composites. An interesting example are Bouligand structures, where each layer of fibers is rotated by a certain angle with respect to the underlying layer, eventually making a complete rotation (Fig. 6e). These effectively helical structures are found in fish scales[59,78–80,139,140] and crustacean exoskeletons (Fig. 6d).[141,142] These structures have been shown to be highly resistant to penetration.[142] Fiber separation within an individual layer during crack propagation in these scales has been modeled using Kendall peeling.[139] Dastjerdi et al. concluded that this localized, less catastrophic peeling failure mode increases the toughness of fish scales and other Bouligand structures, as well as in other layered composites such as nacre. Peeling tests also have been used to assess forces between different constituents in synthetic platelet-based nanocomposites.[143–145] The Barthelat group developed a composite cross-ply glass mimicking the Bouligand structure in fish scales[69] that was 100 times tougher than bulk glass. They showed this both experimentally[139,141] and computationally[69,142] in fish scales and crustacean exoskeletons.

CONCLUSION

How peeling is studied is reviewed herein to gain further understanding of biological adhesives. The two biological adhesive systems that have by far been the most widely studied are featured in detail: the reversible nanostructured adhesive of gecko feet and the permanent fibrous adhesion found in spider silks. In both cases, peeling is a primary failure mode and has provided crucial information about their adhesive behavior. Gecko feet were modeled as pressure-sensitive adhesives, which revealed the effect of the mechanical properties of the adherends, roughness of the substrate, and environmental conditions. These insights have helped to engineer hierarchical adhesive systems mimicking their natural counterparts. Experimental work was carried out with individual setae,[74] but the majority of the work was modeling.

These adhesive systems are still pursued with the goal of improving biomimetic adhesives. Gecko-inspired robots have achieved vertical wall climbing on certain substrates and under varying environmental conditions, but not nearly in the range of different environmental conditions and surfaces as the gecko, yet. Also, neither self-cleaning nor prevention of self-adhesion has been achieved in synthetic systems. Hierarchically structured PSA adhesives inspired by the gecko have shown improved adhesion relative to unstructured PSA, but still cannot match natural gecko feet.

Research of adhesive spider-silk systems is also dominated by modeling work, such as the multiple peeling model. This field provides great potential to engineer robust self-supporting structures using spider-silk-inspired adhesives. Fundamental peeling experiments have systematically determined the humidity response of orb-web adhesion. It might prove fruitful to extend these experiments to more architectures in the future. It is still unknown why only orb-web glues are humidity sensitive despite featuring a composition similar to cobwebs. Spider-silk-inspired adhesives provide significant opportunities for further development. Based on our review, we suggest that more experimental work on biological adhesives might be particularly promising and helpful for the development of broadly applicable bioinspired adhesive systems.

Hierarchical adhesive structures are found on the legs of many insects and spiders but, because of the greater length scale of these features, do not achieve an adhesion as impressive as the gecko. Claws often function in conjunction with hairs to maintain attachment. The Kendall model has been used to model these systems, but because of the oversimplification to a uniform thin film, only a phenomenological understanding has been obtained. This is also the current situation for suction-cup-based adhesive systems such as octopi and mites. These systems have led to an impressive bioinspired adhesive patch with effective resistance to shear-

and peel-failure modes. Lastly, peeling models have been used to study layered composites such as Bouligand structures. Peeling is the toughness increasing mechanism of these structures, and thus has inspired many effective biomimicking materials systems. A further improved theoretical understanding of peeling-mode failure based on first principles for all biological adhesives is likely to accelerate and inspire experimental work and the development of bioinspired adhesives that will outperform current synthetic systems.

ACKNOWLEDGEMENTS

This work was made possible by funding through the National Science Foundation under Grants Nos. DMR-1352542 and DMR-1905902. The authors would like to acknowledge the large amount of constructive feedback obtained from the reviewers during the reviewing stage of this manuscript.

REFERENCES

1. A.V.P.D. Dillard, eds., *Adhesion Science and Engineering: Surfaces, Chemistry and Applications (Annals of Discrete Mathematics)* (Amsterdam: Elsevier, 2002).
2. A.M. Smith, eds., *Biological Adhesives* (Berin: Springer, 2016).
3. K.A. Daltorio, A.D. Horchler, S. Gorb, R.E. Ritzmann, and R.D. Quinn, in *2005 IEEERSJ International Conference* on *Intelligent and Robotic Systems* (IEEE, 2005).
4. A. Asbeck, S. Dastoor, A. Parness, L. Fullerton, N. Esparza, D. Soto, B. Heyneman, and M. Cutkosky, in *2009 IEEE International Conference on Robotics and Automation* (IEEE, 2009).
5. C. Menon, N. Lan, and D. Sameoto, *Appl. Bionics Biomech.* 6, 87 (2009).
6. H. Tao, J.J. Amsden, A.C. Strikwerda, K. Fan, D.L. Kaplan, X. Zhang, R.D. Averitt, and F.G. Omenetto, *Adv. Mater.* 22, 3527 (2010).
7. Y. Wang, J. Guo, L. Zhou, C. Ye, F.G. Omenetto, D.L. Kaplan, and S. Ling, *Adv. Funct. Mater.* 28, 1805305 (2018).
8. T. Siritientong, A. Angspatt, J. Ratanavaraporn, and P. Aramwit, *Pharm. Res.* 31, 104 (2013).
9. P. Aramwit, J. Ratanavaraporn, and T. Siritientong, *Adv. Skin Wound Care* 28, 358 (2015).
10. M.K. Kwak, H.-E. Jeong, and K.Y. Suh, *Adv. Mater.* 23, 3949 (2011).
11. S. Baik, H.J. Lee, D.W. Kim, J.W. Kim, Y. Lee, and C. Pang, *Adv. Mater.* 31, 1803309 (2019).
12. V. Slesarenko, N. Kazarinov, and S. Rudykh, *Smart Mater. Struct.* 26, 035053 (2017).
13. R. Yadav, R. Goud, A. Dutta, X. Wang, M. Naebe, and B. Kandasubramanian, *Ind. Eng. Chem. Res.* 57, 10832 (2018).
14. Z. Qin, B.G. Compton, J.A. Lewis, and M.J. Buehler, *Nat. Commun.* 6, 7038 (2015).
15. D.E. Packham, *Handbook of Adhesion* (Oxford: Wiley-Blackwell, 2005).
16. K. Autumn and J. Puthoff, *Biological Adhesives*, ed. A.M. Smith, 2nd ed. (Berlin: Springer, 2016), pp. 245–280.
17. K. Autumn, *J. Exp. Biol.* 209, 3569 (2006).
18. N.S. Pesika, Y. Tian, B. Zhao, K. Rosenberg, H. Zeng, P. McGuiggan, K. Autumn, and J.N. Israelachvili, *J. Adhes.* 83, 383 (2007).
19. N.N. Ashton, C.-S. Wang, and R.J. Stewart, *Biological Adhesives*, ed. A.M. Smith, 2nd ed. (Berlin: Springer, 2016), pp. 107–128.
20. S. Das and A. Ghosh, *Indian J. Fibre Text. Res.* 34, 31 (2009).
21. J.O. Wolff, M.E. Herberstein, and J.R. Soc, *Interface* 14, 20160783 (2017).
22. Y. Liu, H. Meng, P.B. Messersmith, B.P. Lee, and J.L. Dalsin, *Biological Adhesives*, ed. A.M. Smith, 2nd ed. (Berlin: Springer, 2016), pp. 345–378.
23. W. Yang, G.P. Zhang, X.F. Zhu, X.W. Li, and M.A. Meyers, *J. Mech. Behav. Biomed. Mater.* 4, 1514 (2011).
24. I. Scholz, W.J.P. Barnes, J.M. Smith, and W. Baumgartner, *J. Exp. Biol.* 212, 155 (2008).
25. S.N. Gorb, M. Sinha, A. Peressadko, K.A. Daltorio, and R.D. Quinn, *Bioinspir. Biomim.* 2, S117 (2007).
26. E. Arzt, S. Gorb, and R. Spolenak, *Proc. Natl. Acad. Sci.* 100, 10603 (2003).
27. W. Federle, E.L. Brainerd, T.A. McMahon, and B. Holldobler, *Proc. Natl. Acad. Sci.* 98, 6215 (2001).
28. C.J. Clemente and W. Federle, *Proc. R. Soc. B Biol. Sci.* 275, 1329 (2008).
29. C. Pang, M.K. Kwak, C. Lee, H.E. Jeong, W.-G. Bae, and K.Y. Suh, *Nano Today* 7, 496 (2012).
30. L. Frantsevich, A. Ji, Z. Dai, J. Wang, L. Frantsevich, and S.N. Gorb, *J. Insect Physiol.* 54, 818 (2008).
31. P.N.B. Reis, J.A.M. Ferreira, and F. Antunes, *Int. J. Adhes. Adhes.* 31, 193 (2011).
32. K. Kendall, *J. Phys. Appl. Phys.* 8, 1449 (1975).
33. K.L. Mittal, *Electrocompon. Sci. Technol.* 3, 21 (1976).
34. M.D. Thouless and Q.D. Yang, *Int. J. Adhes. Adhes.* 28, 176 (2008).
35. J.A. Greenwood and J.B.P. Williamson, *Proc. R. Soc. Lond. Ser. Math. Phys. Sci.* 295, 300 (1966).
36. L.F.M. da Silva, R.J.C. Carbas, G.W. Critchlow, M.A.V. Figueiredo, and K. Brown, *Int. J. Adhes. Adhes.* 29, 621 (2009).
37. B.N.J. Persson and M. Scaraggi, *J. Chem. Phys.* 141, 124701 (2014).
38. L. Brely, F. Bosia, and N.M. Pugno, *Bioinspir. Biomim.* 13, 026004 (2018).
39. Z.L. Peng and S.H. Chen, *Phys. Rev. E* 83, 051915 (2011).
40. N. Cañas, M. Kamperman, B. Völker, E. Kroner, R.M. McMeeking, and E. Arzt, *Acta Biomater.* 8, 282 (2012).
41. Z. Peng and S. Chen, *Int. J. Solids Struct.* 60–61, 60 (2015).
42. M. Varenberg, A. Peressadko, S. Gorb, and E. Arzt, *Appl. Phys. Lett.* 89, 121905 (2006).
43. E.M. Moya-Sanz, I. Ivañez, and S.K. Garcia-Castillo, *Int. J. Adhes. Adhes.* 72, 23 (2017).
44. J. Boss, V. Ganesh, and C. Lim, *Compos. Struct.* 62, 113 (2003).
45. V.K. Ganesh and T.S. Choo, *J. Compos. Mater.* 36, 1757 (2002).
46. S. Sun, M. Li, and A. Liu, *Int. J. Adhes. Adhes.* 41, 98 (2013).
47. Z. Peng and S. Chen, *Phys. Rev. E* 91, 042401 (2015).
48. Z. Peng and S. Chen, *Appl. Phys. Lett.* 101, 163702 (2012).
49. B.N.J. Persson, *J. Chem. Phys.* 118, 7614 (2003).
50. Z. Peng, C. Wang, Y. Yang, and S. Chen, *Phys. Rev. E* 94, 10 (2016).
51. Z. Peng and S. Chen, *Colloids Surf. B Biointerfaces* 88, 717 (2011).
52. Z.L. Peng, C. Wang, and S.H. Chen, *Colloids Surf. B Biointerfaces* 122, 662 (2014).
53. Z. Peng, Y. Yang, and S. Chen, *J. Phys. Appl. Phys.* 50, 315402 (2017).
54. A. Aggarwal, S. Ramakrishna, and V.K. Ganesh, *J. Compos. Mater.* 35, 665 (2001).
55. C. Ayranci and J. Carey, *Compos. Struct.* 85, 43 (2008).
56. J. Tate, A. Kelkar, and J. Whitcomb, *Int. J. Fatigue* 28, 1239 (2006).
57. J. Chopin, R. Villey, D. Yarusso, E. Barthel, C. Creton, and M. Ciccotti, *Macromolecules* 51, 8605 (2018).
58. F. Sosson, A. Chateauminois, and C. Creton, *J. Polym. Sci. B Polym. Phys.* 43, 3316 (2005).
59. S.E. Naleway, M.M. Porter, J. McKittrick, and M.A. Meyers, *Adv. Mater.* 27, 5455 (2015).
60. S. Gorb, M. Varenberg, A. Peressadko, J. Tuma, and J.R. Soc, *Interface* 4, 271 (2006).

61. D. Brodoceanu, C.T. Bauer, E. Kroner, E. Arzt, and T. Kraus, *Bioinspir. Biomim.* 11, 051001 (2016).
62. Z.L. Peng, S.H. Chen, and A.K. Soh, *Int. J. Solids Struct.* 47, 1952 (2010).
63. S.R. Koebley, F. Vollrath, and H.C. Schniepp, *Mater. Horiz.* 4, 377 (2017).
64. A. Meyer, N.M. Pugno, S.W. Cranford, and J.R. Soc, *Interface* 11, 20140561 (2014).
65. N.M. Pugno, S.W. Cranford, and M.J. Buehler, *Small* 9, 2747 (2013).
66. P.H. Niewiarowski, A.Y. Stark, and A. Dhinojwala, *J. Exp. Biol.* 219, 912 (2016).
67. N.N. Ashton, D.S. Taggart, and R.J. Stewart, *Biopolymers* 97, 432 (2011).
68. S.N. Gorb, *Am. Entomol.* 51, 31 (2005).
69. Z. Yin, A. Dastjerdi, and F. Barthelat, *Acta Biomater.* 75, 439 (2018).
70. Z. Peng, C. Wang, L. Chen, and S. Chen, *Int. J. Solids Struct.* 51, 4596 (2014).
71. L. He, J. Lou, S. Kitipornchai, J. Yang, and J. Du, *Int. J. Solids Struct.* 167, 184 (2019).
72. D. Jain, T.A. Blackledge, T. Miyoshi, and A. Dhinojwala, *Biological Adhesives*, ed. A.M. Smith, 2nd ed. (Berlin: Springer, 2016), pp. 303–319.
73. Z. Gu, S. Li, F. Zhang, and S. Wang, *Adv. Sci.* 3, 1500327 (2016).
74. K. Autumn, Y.A. Liang, S.T. Hsieh, W. Zesch, W.P. Chan, T.W. Kenny, R. Fearing, and R.J. Full, *Nature* 405, 681 (2000).
75. G. Huber, S.N. Gorb, R. Spolenak, and E. Arzt, *Biol. Lett.* 1, 2 (2005).
76. G. Greco, M.F. Pantano, B. Mazzolai, and N.M. Pugno, *Sci. Rep.* 9, 5776 (2019).
77. G. Amarpuri, C. Zhang, C. Diaz, B.D. Opell, T.A. Blackledge, and A. Dhinojwala, *ACS Nano* 9, 11472 (2015).
78. Y. Bouligand, *Tissue Cell* 4, 189 (1972).
79. A. Bigi, M. Burghammer, R. Falconi, M.H.J. Koch, S. Panzavolta, and C. Riekel, *J. Struct. Biol.* 136, 137 (2001).
80. E.A. Zimmermann, B. Gludovatz, E. Schaible, N.K.N. Dave, W. Yang, M.A. Meyers, and R.O. Ritchie, *Nat. Commun.* 4, 2634 (2013).
81. H. Hertz, *J. Reine Angew. Math.* 92, 156 (1881).
82. M.S. Stanislav and S.N. Gorb, *Biological Micro- and Nanotribology* (Berlin: Springer, 2001).
83. K.L. Johnson, K. Kendall, and A.D. Roberts, *Proc. R. Soc. Math. Phys. Eng. Sci.* 324, 301 (1971).
84. B.V. Derjaguin, V.M. Muller, and Y.P. Toporov, *J. Colloid Interface Sci.* 53, 314 (1975).
85. V.M. Muller, V.S. Yushchenko, and B.V. Derjaguin, *J. Colloid Interface Sci.* 77, 91 (1980).
86. R. Spolenak, S. Gorb, H. Gao, and E. Arzt, *Proc. R. Soc. Math. Phys. Eng. Sci.* 461, 305 (2005).
87. D.H. Kaelble, *J. Adhes.* 37, 205 (1992).
88. M. Ciccotti, B. Giorgini, D. Vallet, and M. Barquins, *Int. J. Adhes. Adhes.* 24, 143 (2004).
89. N.M. Pugno, *Int. J. Fract.* 171, 185 (2011).
90. L. Brely, F. Bosia, S. Palumbo, M. Fraldi, A. Dhinojwala, N.M. Pugno, and J.R. Soc, *Interface* 16, 20190388 (2019).
91. T. Tang, C.-Y. Hui, N.J. Glassmaker, and J.R. Soc, *Interface* 2, 505 (2005).
92. A. Jagota and S.J. Bennison, *Integr. Comp. Biol.* 42, 1140 (2002).
93. K. Autumn, *Integr. Comp. Biol.* 42, 1081 (2002).
94. B.N.J. Persson and S. Gorb, *J. Chem. Phys.* 119, 11437 (2003).
95. L. Afferrante, G. Carbone, G. Demelio, and N. Pugno, *Tribol. Lett.* 52, 439 (2013).
96. M.R. Begley, R.R. Collino, J.N. Israelachvili, and R.M. McMeeking, *J. Mech. Phys. Solids* 61, 1265 (2013).
97. J.A. Williams and J.J. Kauzlarich, *Tribol. Int.* 38, 951 (2005).
98. M. Zhou, Y. Tian, N. Pesika, H. Zeng, J. Wan, Y. Meng, and S. Wen, *J. Adhes.* 87, 1045 (2011).
99. C. Derail, A. Allal, G. Marin, and P. Tordjeman, *J. Adhes.* 61, 123 (1997).
100. Y. Tian, N. Pesika, H. Zeng, K. Rosenberg, B. Zhao, P. McGuiggan, K. Autumn, and J. Israelachvili, *Proc. Natl. Acad. Sci.* 103, 19320 (2006).
101. G. Huber, S. Gorb, N. Hosoda, R. Spolenak, and E. Arzt, *Acta Biomater.* 3, 607 (2007).
102. A.N. Gent and R.P. Petrich, *Proc. R. Soc. Math. Phys. Eng. Sci.* 310, 433 (1969).
103. A.N. Gent and A.J. Kinloch, *J. Polym. Sci. Part-2 Polym. Phys.* 9, 659 (1971).
104. K. Autumn, *J. Exp. Biol.* 209, 260 (2006).
105. G. Haiat and E. Barthel, *Langmuir* 23, 11643 (2007).
106. A.Y. Stark and C.T. Mitchell, *Integr. Comp. Biol.* 59, 214 (2019).
107. K. Autumn, M. Sitti, Y.A. Liang, A.M. Peattie, W.R. Hansen, S. Sponberg, T.W. Kenny, R. Fearing, J.N. Israelachvili, and R.J. Full, *Proc. Natl. Acad. Sci.* 99, 12252 (2002).
108. M.P. Murphy, S. Kim, M. Sitti, and A.C.S. Appl, *Mater. Interfaces* 1, 849 (2009).
109. J.O. Wolff and S.N. Gorb, *Attach. Struct. Adhes. Secret. Arachn.* 7, 79 (2016).
110. L. Ge, S. Sethi, L. Ci, P.M. Ajayan, and A. Dhinojwala, *Proc. Natl. Acad. Sci.* 104, 10792 (2007).
111. H. Lee, B.P. Lee, and P.B. Messersmith, *Nature* 448, 338 (2007).
112. Y. Mengüç, S.Y. Yang, S. Kim, J.A. Rogers, and M. Sitti, *Adv. Funct. Mater.* 22, 1246 (2012).
113. B. Soltannia, D. Sameoto, and A.C.S. Appl, *Mater. Interfaces* 6, 21995 (2014).
114. H. Yi, S.H. Lee, M. Seong, M.K. Kwak, and H.E. Jeong, *J. Mater. Chem. B* 6, 8064 (2018).
115. J. Lee and R.S. Fearing, *Langmuir* 24, 10587 (2008).
116. V. Alizadehyazdi, A. Simaite, M. Spenko, and A.C.S. Appl, *Mater. Interfaces* 11, 8654 (2019).
117. Z. Yan, F. Zhang, J. Wang, F. Liu, X. Guo, K. Nan, Q. Lin, M. Gao, D. Xiao, Y. Shi, Y. Qiu, H. Luan, J.H. Kim, Y. Wang, H. Luo, M. Han, Y. Huang, Y. Zhang, and J.A. Rogers, *Adv. Funct. Mater.* 26, 2629 (2016).
118. H.C. Schniepp, S.R. Koebley, and F. Vollrath, *Adv. Mater.* 25, 7028 (2013).
119. F.G. Omenetto and D.L. Kaplan, *Science* 329, 528 (2010).
120. F. Chen, D. Porter, and F. Vollrath, *Acta Biomater.* 8, 2620 (2012).
121. J. Zhang, J. Kaur, R. Rajkhowa, J.L. Li, X.Y. Liu, and X.G. Wang, *Mater. Sci. Eng. C* 33, 3206 (2013).
122. Q. Wang and H.C. Schniepp, *ACS Macro Lett.* 7, 1364 (2018).
123. S. Roh, A.H. Williams, R.S. Bang, S.D. Stoyanov, and O.D. Velev, *Nat. Mater.* 18, 1315 (2019).
124. B.D. Opell and M.L. Hendricks, *J. Exp. Biol.* 210, 553 (2007).
125. B.D. Opell, S.E. Karinshak, and M.A. Sigler, *J. Exp. Biol.* 216, 3023 (2013).
126. V. Sahni, T.A. Blackledge, and A. Dhinojwala, *Nat. Commun.* 1, 19 (2010).
127. D. Jain, C. Zhang, L.R. Cool, T.A. Blackledge, C. Wesdemiotis, T. Miyoshi, and A. Dhinojwala, *Biomacromol* 16, 3373 (2015).
128. V. Sahni, J. Harris, T.A. Blackledge, and A. Dhinojwala, *Nat. Commun.* 3, 1106 (2012).
129. Y. Guo, Z. Chang, B. Li, Z.-L. Zhao, H.-P. Zhao, X.-Q. Feng, and H. Gao, *Appl. Phys. Lett.* 113, 103701 (2018).
130. A.O. Krushynska, F. Bosia, M. Miniaci, and N.M. Pugno, *New J. Phys.* 19, 105001 (2017).
131. M. Miniaci, A. Krushynska, A.B. Movchan, F. Bosia, and N.M. Pugno, *Appl. Phys. Lett.* 109, 071905 (2016).
132. E. Blasingame, T. Tuton-Blasingame, L. Larkin, A.M. Falick, L. Zhao, J. Fong, V. Vaidyanathan, A. Visperas, P. Geurts, X. Hu, C.L. Mattina, and C. Vierra, *J. Biol. Chem.* 284, 29097 (2009).
133. K. Singha, S. Maity, and M. Singha, *Front. Sci.* 2, 92 (2012).

134. I. Özdemir, *Acta Mech.* 228, 1735 (2017).
135. L. Heepe, D.S. Petersen, L. Tölle, J.O. Wolff, and S.N. Gorb, *Bio-inspired Structured Adhesives* (Berlin: Springer, 2017), pp. 47–61.
136. J.O. Wolff and S.N. Gorb, *Bio-inspired Systems* (Berlin: Springer, 2016), pp. 87–93.
137. D.W. Kim, S. Baik, H. Min, S. Chun, H.J. Lee, K.H. Kim, J.Y. Lee, and C. Pang, *Adv. Funct. Mater.* 29, 1807614 (2019).
138. F. Meng, Q. Liu, X. Wang, D. Tan, L. Xue, and W.J.P. Barnes, *Philos. Trans. R. Soc. Math. Phys. Eng. Sci.* 377, 20190131 (2019).
139. A.K. Dastjerdi and F. Barthelat, *J. Mech. Behav. Biomed. Mater.* 52, 95 (2015).
140. Y.S. Lin, C.T. Wei, E.A. Olevsky, and M.A. Meyers, *J. Mech. Behav. Biomed. Mater.* 4, 1145 (2011).
141. L.K. Grunenfelder, N. Suksangpanya, C. Salinas, G. Milliron, N. Yaraghi, S. Herrera, K. Evans-Lutterodt, S.R. Nutt, P. Zavattieri, and D. Kisailus, *Acta Biomater.* 10, 3997 (2014).
142. N. Suksangpanya, N.A. Yaraghi, D. Kisailus, and P. Zavattieri, *J. Mech. Behav. Biomed. Mater.* 76, 38 (2017).
143. M. Cai, A.J. Glover, T.J. Wallin, D.E. Kranbuehl, and H.C. Schniepp, *AIP Conf. Proc.* 1255, 95 (2010).
144. L.R. Dickinson, D.E. Kranbuehl, and H.C. Schniepp, *Surf. Innov.* 4, 158 (2016).
145. D.E. Kranbuehl, M. Cai, A.J. Glover, and H.C. Schniepp, *J. Appl. Polym. Sci.* 122, 3739 (2011).